

Article

Alkylated Polyphenyl Ethers as High-Performance Synthetic Lubricants

Renguo Lu ^{1,*} , Hiroshi Tani ¹, Shinji Koganezawa ¹ and Masayuki Hata ²¹ Faculty of Engineering Science, Kansai University, Osaka 564-8680, Japan² MORESCO Corporation, Hyogo 650-0047, Japan

* Correspondence: r_lu@kansai-u.ac.jp; Tel.: +81-6-6368-0781

Abstract: Lubricants exhibiting both thermal and chemical stability that consequently generate less hydrogen during friction are required to avoid the hydrogen embrittlement of moving mechanical components. The present work studied the effects of the length and number of alkyl chains on the tribological properties of polyphenyl ethers (PPEs), which feature good thermal and radiation resistance. PPEs were found to have much lower friction coefficients compared with a poly-alpha-olefin and alkyl diphenyl ether, and the effect of the running-in process on friction appeared to be negligible. The formation of polymers on the friction track evidently decreased the friction coefficients of the lubricants and the wear rates were almost zero for all the PPEs, indicating excellent anti-wear properties. Analyses with a quadrupole mass spectrometer connected to a friction tester under vacuum indicated negligible hydrogen generation from 4P2E, which had no alkyl chains, after the running-in. R1-4P2E, having a C₁₆H₃₃ chain, showed hydrogen desorption similar to that of the alkyl diphenyl ether, which had a C₁₈H₃₇ alkyl chain. R2-4P2E, with two C₁₆H₃₃ chains, produced significant hydrogen, but with a long induction period; thus, it provided good wear protection. Although alkyl chains increased the risk of hydrogen generation, PPEs with such chains may have applications as standard lubricants.

Keywords: polyphenol ether; chemical structure; tribochemical decomposition; hydrogen generation; chemical stability



Citation: Lu, R.; Tani, H.; Koganezawa, S.; Hata, M. Alkylated Polyphenyl Ethers as High-Performance Synthetic Lubricants. *Lubricants* **2022**, *10*, 275.

<https://doi.org/10.3390/lubricants10100275>

Received: 29 September 2022

Accepted: 20 October 2022

Published: 21 October 2022

Publisher's Note: MDPI stays neutral with regard to jurisdictional claims in published maps and institutional affiliations.



Copyright: © 2022 by the authors. Licensee MDPI, Basel, Switzerland. This article is an open access article distributed under the terms and conditions of the Creative Commons Attribution (CC BY) license (<https://creativecommons.org/licenses/by/4.0/>).

1. Introduction

Any mechanical device that involves movement will encounter friction, which consumes a significant amount of energy. The wear induced by friction is also a major cause of mechanical failure. In fact, it has been estimated that more than one third of the energy used worldwide is consumed by friction in various forms. To minimize these costs, lubrication science has been focused on reducing friction, minimizing wear, evacuating heat, and removing contaminants. However, it is well known that lubricants can undergo thermal decomposition in response to the heat of friction or high operating temperatures, as well as tribochemical decomposition induced by the high activity of nascent steel surfaces [1–5]. It has been suggested that hydrogen generated by lubricant decomposition is also an important aspect of the hydrogen embrittlement of metal parts. As an example, this phenomenon can decrease the rolling fatigue life of bearings [6–9].

Some efforts have been made to control lubricant decomposition during friction. Various additives containing sulfur or phosphorous have been shown to reduce the tribochemical decomposition of MAC oil (1,2,4-tris(2-octyldodecyl) cyclopentane) by deactivating nascent steel surfaces [10]. Extreme pressure additives and antiwear additives can also inhibit hydrogen diffusion and reduce the appearance of white etching crack formations by providing a thin Zn-S dominated tribofilm [11]. Despite this, an increasing focus on environmental protection has led to new challenges related to lubricant science, such as by restricting the use of elements, including phosphorus and sulfur, or chlorinated additives [12]. In fact, the most popular additive, zinc dialkyldithiophosphate, is phytotoxic,

and plants that accumulate this compound through root absorption or deposition can pose health risks to consumers [13]. It is likely that only environmentally acceptable lubricants or additives will be available in the near future.

Lubricants that exhibit superior thermal and chemical stabilities have been found to generate less hydrogen during friction. Examples include ionic liquids, such as 1-ethyl-3-methylimidazolium bis(trifluoromethylsulfonyl) imide and 1-dodecyl-3-methylimidazolium bis(trifluoromethylsulfonyl) imide, which produce much less hydrogen during friction comparing with MAC [14]. However, both expense and environmental restrictions limit the application of ionic liquids. Alkyldiphenyl ethers (ADEs) have been shown to generate negligible amounts of hydrogen even after long durations of friction under vacuum [15] and have been used as base oils in bearing grease formulations [16]. Longer alkyl chains and greater numbers of such chains decrease the friction coefficients of ADEs; however, the wear-reducing properties must be improved. Compared with ADEs, polyphenyl ethers (PPEs) show significantly superior thermal and chemical stabilities, as well as radiation resistance [17–21]. A 5P4E (5 phenyl 4 ether)-based lubricant has been employed in gas turbine engines [22,23] and its rheologic properties have been studied in elastohydrodynamic lubrication [24,25]. Even so, the disadvantages of 5P4E, such as relatively poor tribological properties and a high pour point, limit its applications [26]. Despite this, the alkylation of aromatic compounds could potentially generate compounds suitable as lubricants [27]; thus, the tribological properties of PPEs should be improved.

On this basis, the objective of the present work was to evaluate the effects of both the lengths of alkyl chains and the number of alkyl chains on the tribological properties, and tribochemical decomposition of PPEs.

2. Materials and Methods

2.1. Lubricants

PPEs (MORESCO Corporation, Kobe, Japan) having different alkyl chain lengths and varying numbers of attached alkyl chains were obtained for evaluation. The molecular structures of these compounds are provided in Figure 1. In each case, these PPEs contained straight alkyl chains. The phenyl rings in these molecules provided chemical stability, while adjusting the alkyl chain length and the number of attached chains allowed the molecular flexibility to be tuned. Table 1 summarizes the typical physical properties of the various samples. An ADE having a C18 alkyl chain (MORESCO Corporation, Kobe, Japan) was used as a reference to evaluate the difference between PPEs and ADEs. A poly- α -olefin (PAO30, MORESCO Corporation, Kobe, Japan) was also used as a reference. All the physical properties listed in Table were tested in MORESCO Corporation, Kobe, Japan.

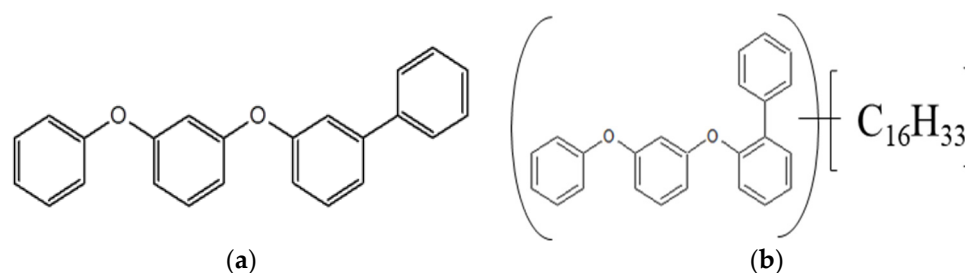


Figure 1. Cont.

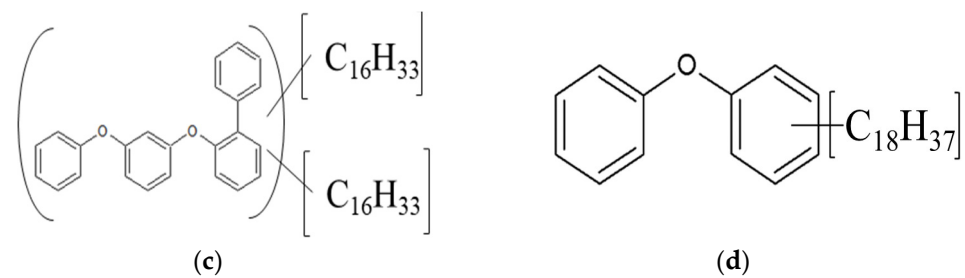


Figure 1. Molecular structures of the PPEs (a) 4P2E, (b) R1-4P2E, and (c) R2-4P2E, and of the (d) C18 ADE.

Table 1. Physical properties of the lubricants evaluated in this work.

Physical Properties	4P2E	R1-4P2E	R2-4P2E	ADE (C18)
Density (15 °C $\text{g}\cdot\text{cm}^{-3}$)	1.167	1.014	0.952	0.928
40 °C viscosity ($\text{mm}^2\cdot\text{s}^{-1}$)	125	240	410	26.1
Viscosity index	−103	32	90	110
Flash point (°C)	260	308	334	250
Pour point (°C)	2.5	−15	−20	−50

2.2. Tribological Tests

A reciprocating ball-on-disk friction tester (Heidon-14DR, SHINTO Scientific Co., Ltd., Tokyo, Japan), illustrated in Figure 2, was used to ascertain friction coefficients. The ball in this device was made of AISI 52100 steel and had a diameter of 6.35 mm and hardness of HRC65. An AISI 52100 steel disk having a hardness of HRC55 and polished to a surface roughness of 0.015 was also used. A load of 10 N was applied with a movement rate of $8.0 \text{ mm}\cdot\text{s}^{-1}$, sliding stroke of 4 mm, and test duration of 1 h. All tribological tests were carried out under ambient conditions ($23 \pm 2 \text{ }^\circ\text{C}$, relative humidity of 45–55%) and repeated at least three times for a given test condition.

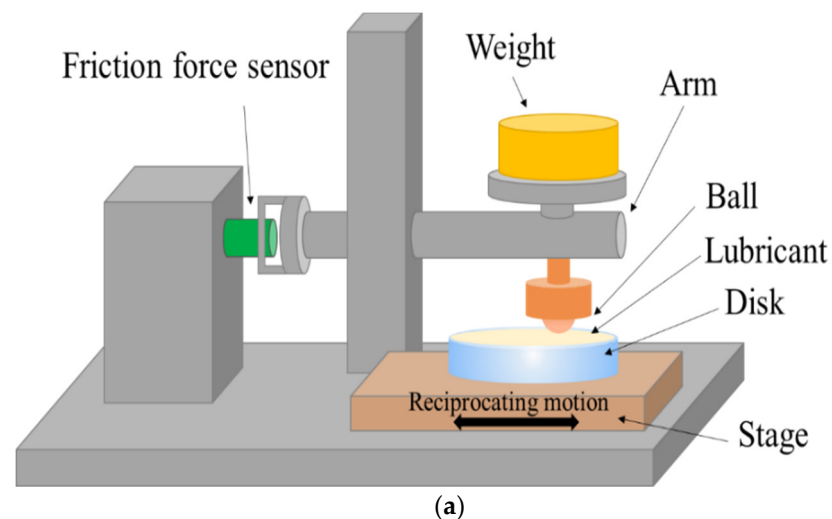


Figure 2. Cont.

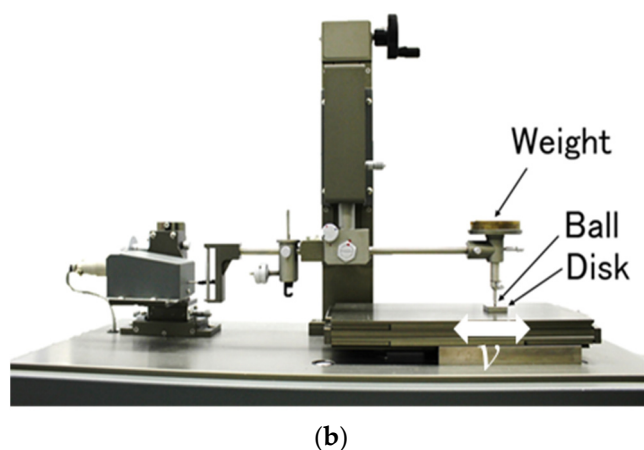


Figure 2. (a) Schematic diagram and (b) physical picture of the reciprocating friction tester.

2.3. Measurement of Gaseous Products Generated by Lubricant Decomposition

A ball-on-disk friction tester installed in a high vacuum chamber was connected to a quadrupole mass spectrometer (Q-mass, M-201QA-TDM, Canon Anelva Corporation, Kawasaki, Japan) to monitor the gaseous products generated by lubricant decomposition, as shown in Figure 3. The ball was made of AISI 52100 steel and had a diameter of 6.35 mm and hardness of HRC65. The disk was mounted on a drive shaft rotated by a magnetic drive assembly. Preliminary trials showed that it was not possible to observe the tribochemical decomposition of PPEs when using an AISI 52100 steel disk with a hardness of HRC55 because overly long durations were required to stimulate the formation of a nascent surface in the case that PPEs were used as lubricants. During these trials, the bearings in the magnetic drive assembly would fail before the formation of the nascent surface. Thus, to accelerate the appearance of a nascent surface, the disk was first annealed at 750 °C such that its hardness was decreased to HRC20.

Adsorbed water was removed from the main chamber by heating the device for 8 h at 100 °C, after which the disk surface was coated with lubricant to an average thickness of 10 µm under a nitrogen atmosphere. The chamber was subsequently evacuated to a stable pressure of less than 8×10^{-5} Pa and the friction test was carried out. The load during these experiments was 5.4 N and the sliding speed was $30 \text{ mm} \cdot \text{s}^{-1}$. Gaseous products arising from the decomposition of the lubricant during friction could be analyzed by the Q-mass instrument.

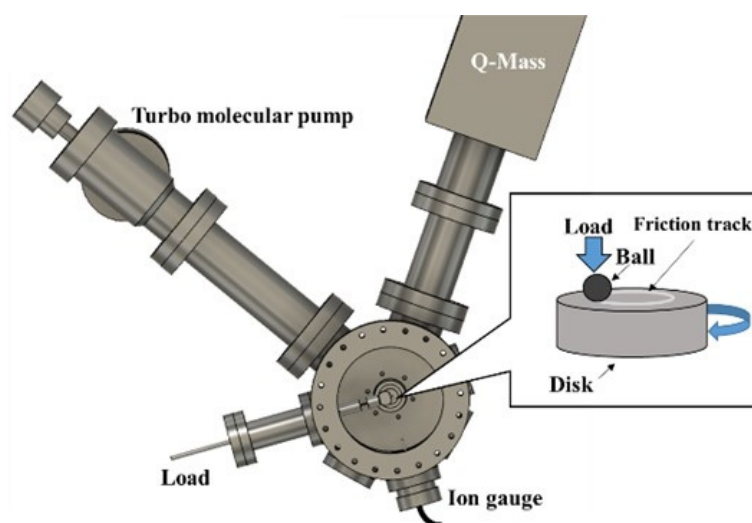


Figure 3. A diagram of the apparatus used to determine the gaseous products generated by lubricant decomposition.

Because the Q-mass required a high vacuum during the analysis of these gaseous products, the PAO sample could not be evaluated as a result of its high vapor pressure. Therefore, a synthetic hydrocarbon oil (MAC oil, Nye Lubricants, Inc., Fairhaven, MA, USA) that is often used in space environments and vacuum systems was instead employed as the reference lubricant.

2.4. Characterization

Following the friction tests, the test pieces were rinsed with hexane to remove the excess lubricant. The wear tracks on the disks and balls were subsequently observed and the surface profiles were measured using a confocal laser scanning microscope (OLS5000, Olympus, Tokyo, Japan). The tribofilm formed on each friction track was also analyzed by micro-Raman spectroscopy (XploRA, Horiba Ltd., Kyoto, Japan), employing a laser wavelength of 532 nm and optical filter setting of 1%.

3. Results and Discussion

3.1. Tribological Properties of Polyphenyl Ethers

Typical friction curves acquired using the reciprocating ball-on-disk friction tester are presented in Figure 4. The PAO was found to have the highest friction coefficient and its coefficient was also obviously increased because of the effect of the running-in process. The friction coefficient of the ADE was lower and only a slight increase was noted throughout the running-in process. Although the absolute friction coefficients of the PAO and ADE were lower than those reported in a previous paper [28], the basic trends exhibited by the data were the same. The difference between the present work and prior research can possibly be attributed to variations in the hardness of the test pieces. Moreover, all the PPE samples showed much lower friction coefficients compared with the PAO and ADE. The effects of the running-in process on the friction values for these specimens were also negligible because the friction coefficients were stable. Furthermore, R1-4P2E and R2-4P2E showed a lower friction coefficient than 4P2E, suggesting alkylation could decrease the friction coefficient, which was similar to the report in ADEs [28]. No obvious difference in the friction coefficient between R1-4P2E and R2-4P2E was observed. The reasons still remained unclear; however, possibly as a consequence of the relatively low load. In this case, a thick lubricant film could be formed because of their high viscosity.

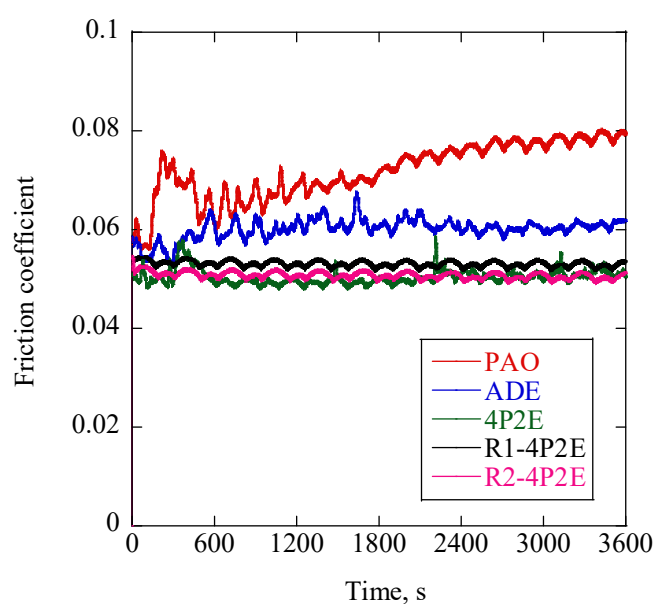


Figure 4. Variations in friction coefficients over time for the various lubricants.

Figure 5 provides photographs and surface profiles of the wear scars on balls and disks. Both the diameter of the wear scar on the balls and the wear scar width on disks decreased when the PPEs were used. However, it was not possible to quantitatively ascertain the wear rates of the disks because the wear depths were not clear, as is apparent from the surface profiles. Instead, the wear rates of the balls were calculated from the worn volumes based on measurements of the surface profiles. Figure 6 shows a cross section of a typical ball. The worn volume, V , was obtained from the equation

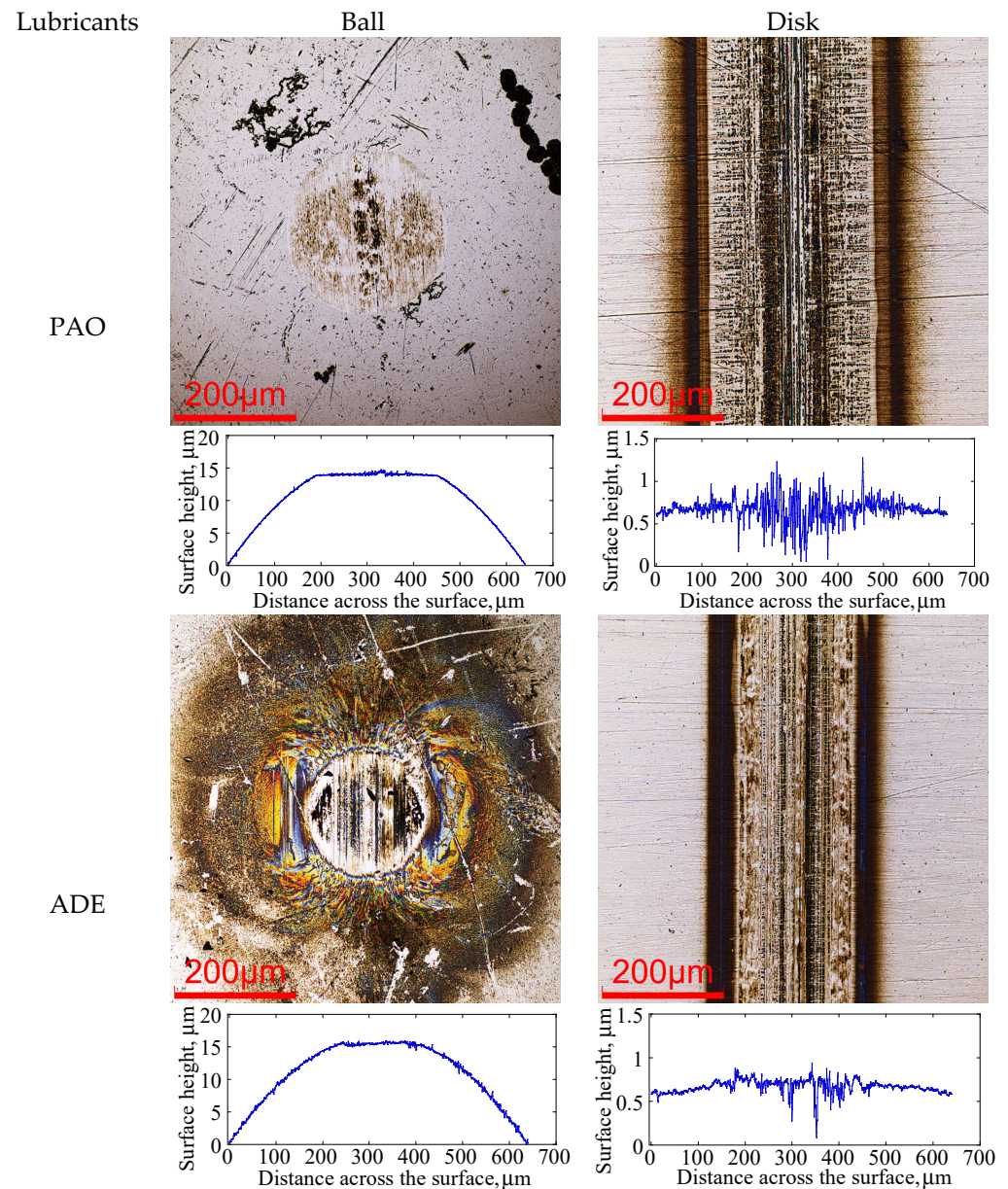


Figure 5. Cont.

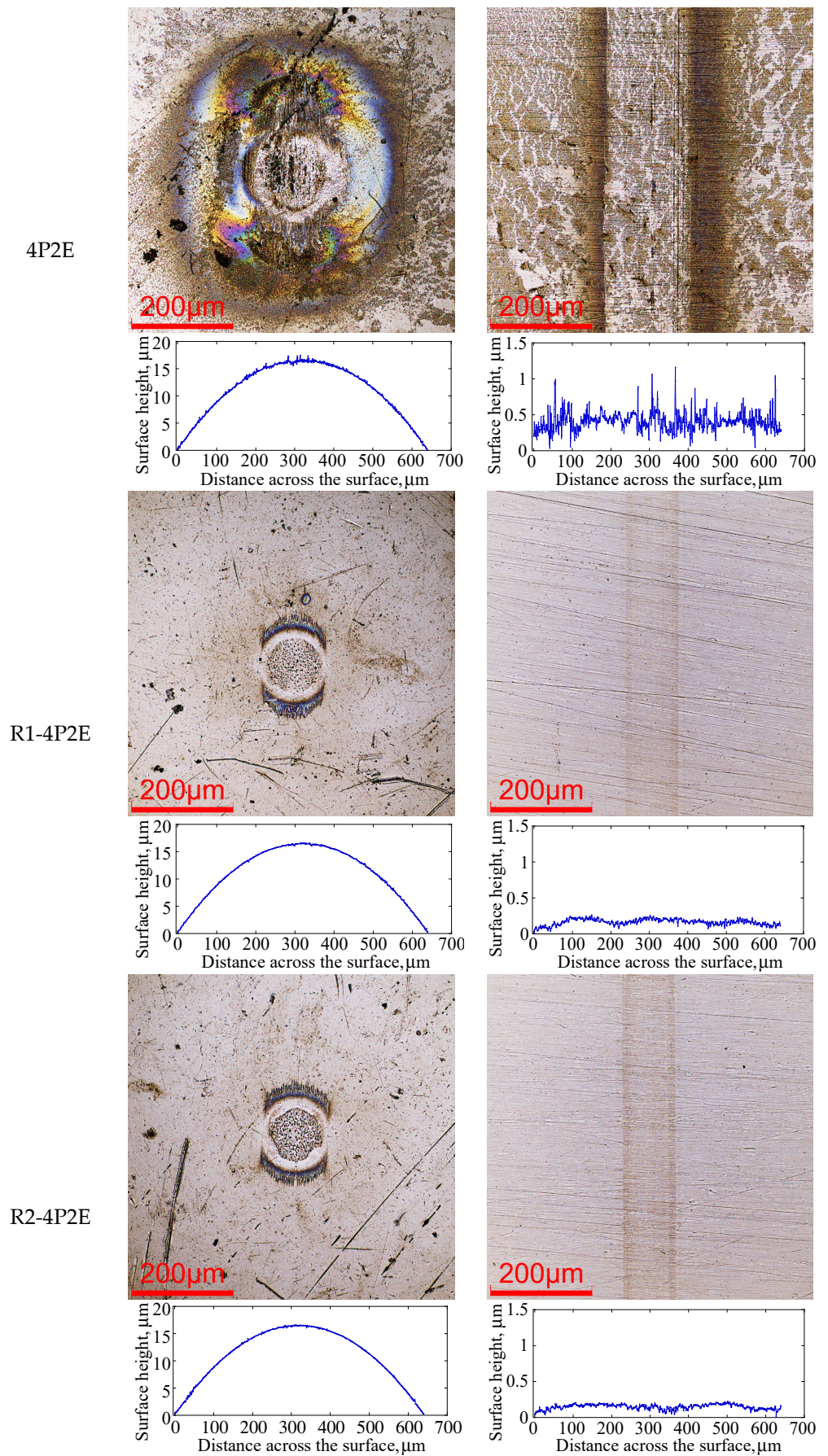


Figure 5. Photographs and surface profiles of wear scars on balls and disks.

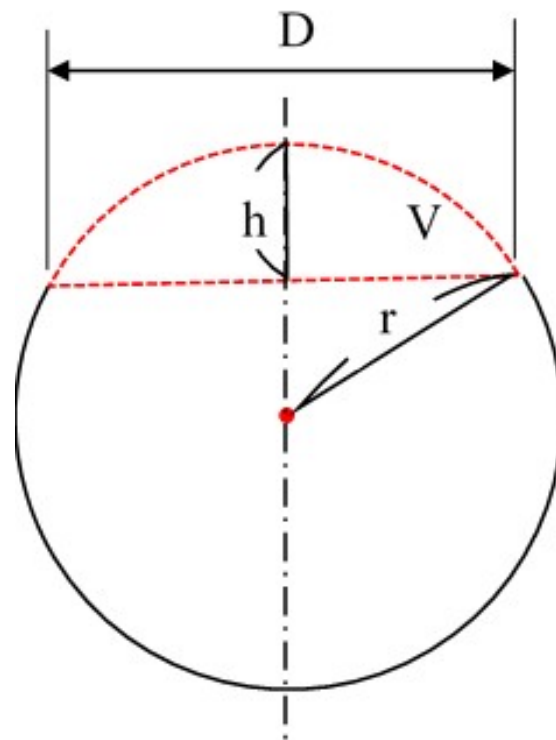


Figure 6. A diagram of the cross section of a ball used in friction tests.

$$V = \frac{h \cdot \pi}{6} \times \left(3 \left(\frac{D}{2} \right)^2 + h^2 \right) \quad (1)$$

where D is the diameter of the worn surface and h is the height of the lost portion. This value was, in turn, defined as

$$h = r - \sqrt{r^2 - \left(\frac{D}{2} \right)^2} \quad (2)$$

in which r is the radius of the ball.

The wear rate, R ($\mu\text{m}^3/(\text{N}\cdot\text{m})$), was defined as

$$R = \frac{V}{W \cdot L} \quad (3)$$

where W is the load and L is the sliding distance.

The calculated wear rates and the average friction coefficients determined for the lubricants are summarized in Figure 7. Although wear scar appeared on the balls (as can be seen in Figure 5), the calculated wear rates were almost zero for all the PPEs. The high viscosities of these materials are thought to have provided sufficient lubrication between the friction pairs, preventing wearing of the surfaces. Typically, a high-viscosity lubricant will increase the friction; however, in this case, the PPEs showed lower friction coefficients than the ADE and PAO.

The mechanism by which the PPEs provided reduced friction was assessed by performing a Raman analysis and typical Raman spectra acquired from the bulk lubricants, and the friction track, as shown in Figure 8. Two broad peaks, at 1560 and 1360 cm^{-1} , were obtained from the friction track. Although these could be assigned to the G band corresponding to the stretching vibrations of sp^2 hybridized carbons and the D band resulting from the breathing mode of sp^3 hybridized ring carbons [29–32], it was difficult to prove the formation of diamond-like carbon. In addition, a peak corresponding to $=\text{CH}_2$ bending can be seen near 1350 cm^{-1} and a $\text{C}=\text{C}$ stretching vibration appears near 1590 cm^{-1} [33,34]. There-

fore, high-molecular-weight hydrocarbons, traditionally referred to as friction polymers, were evidently formed on the friction surface and served to decrease the friction coefficient.

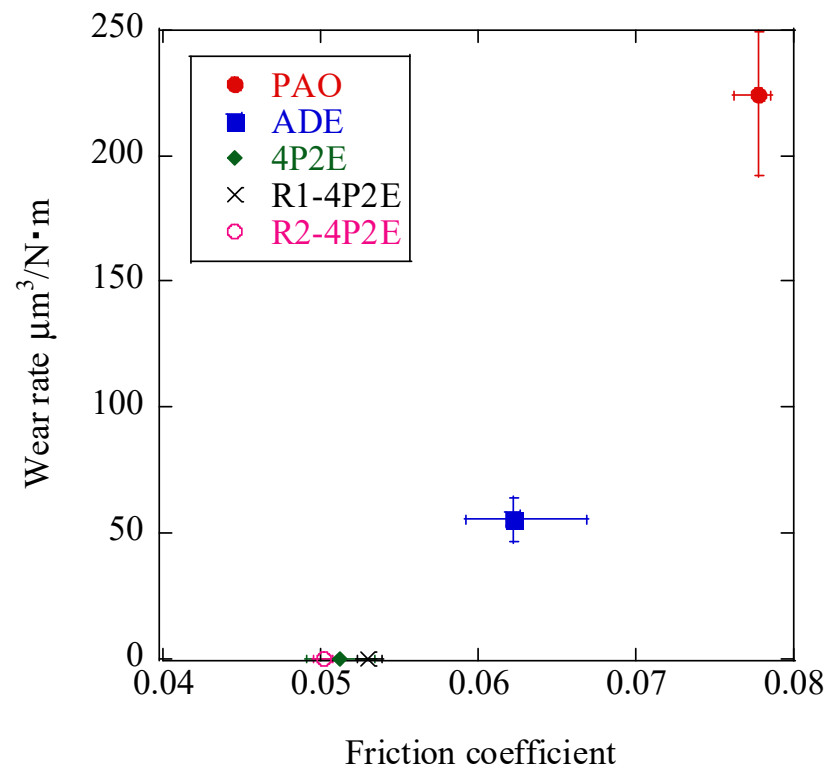


Figure 7. Wear rates as functions of the friction coefficients.

Although this study did not observe obvious differences in the friction coefficients and wear rates for PPEs having different alkyl chains, possibly as a consequence of the relatively low load that was applied, these alkyl chains increased the mobility of the PPEs (as shown in Table 1) and would be expected to allow the application of these materials as standard lubricants.

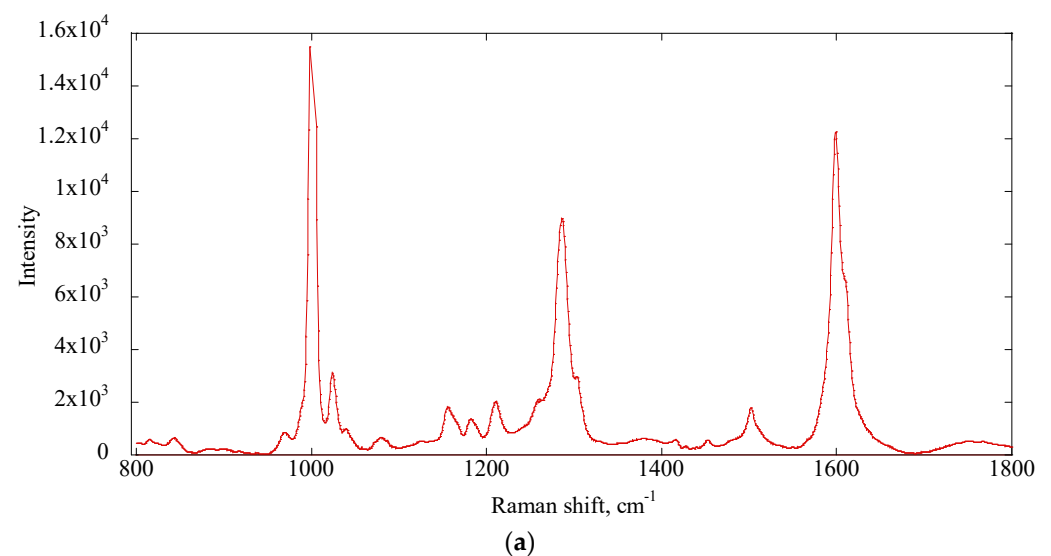


Figure 8. Cont.

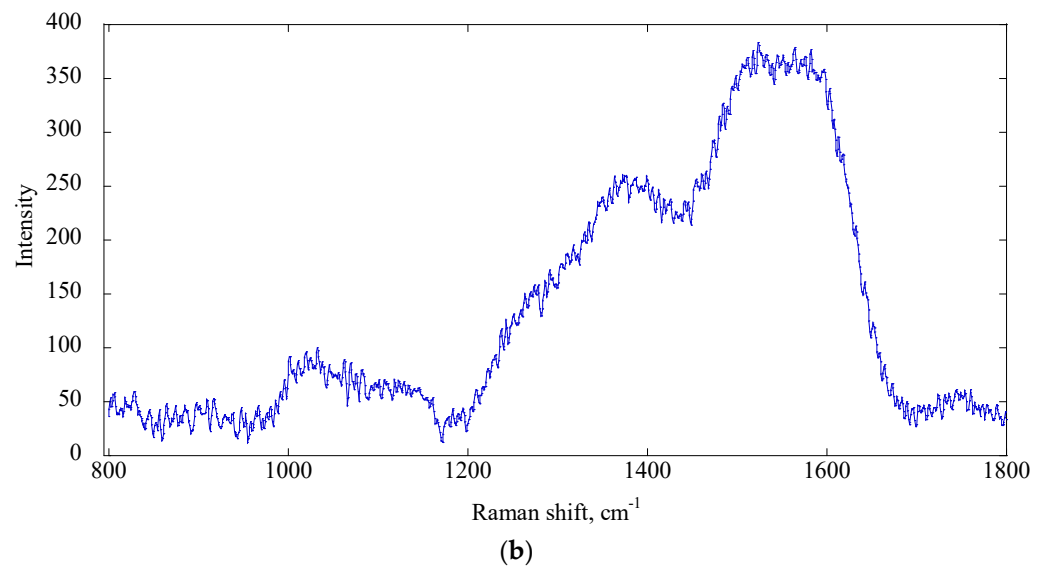


Figure 8. Raman spectra obtained from (a) the lubricant 4P2E in bulk and (b) the friction track.

3.2. Tribochemical Decomposition of Polyphenyl Ethers

Figure 9 presents the typical mass spectra obtained from the decomposed 4P2E, indicating the generation of hydrogen and gaseous low-molecular-weight hydrocarbons. The C_6H_5 and C_6H_5O fragments produced from the phenyl ether groups provide direct evidence for the tribochemical decomposition of the lubricant as a result of friction. As noted, these fragments can polymerize to form friction polymers.

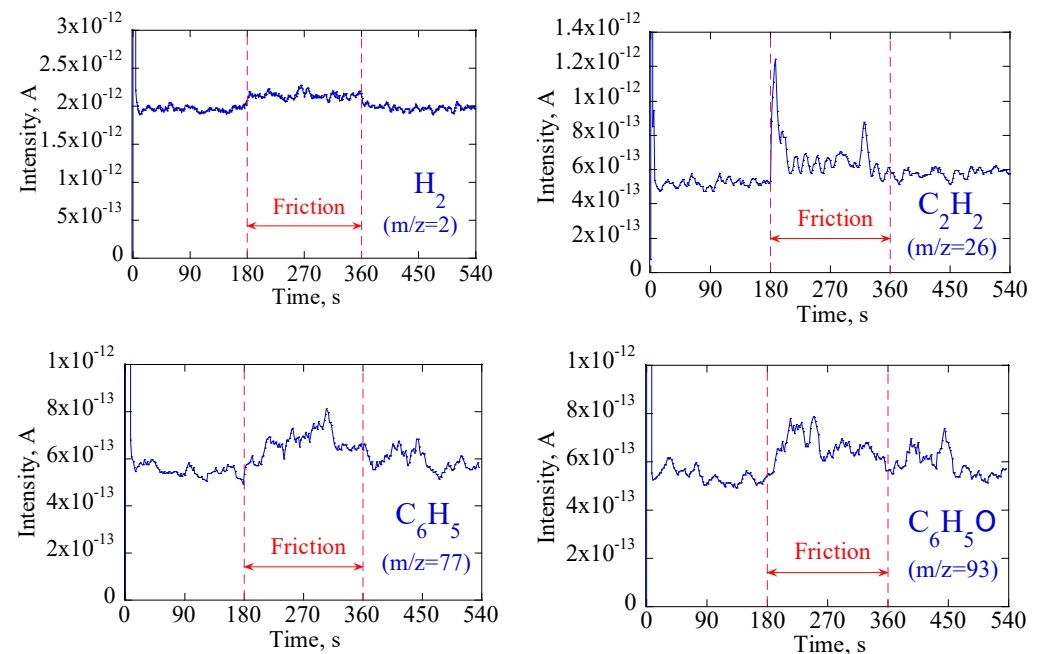


Figure 9. Typical mass spectra obtained from lubricant 4P2E.

The desorption rate, R_d , of these gaseous products was calculated as

$$R_d = \frac{C \cdot \Delta P}{k \cdot T \cdot v \cdot d} \quad (4)$$

where C is the conductance at the outlet of the vacuum chamber, k is Boltzmann's constant, T is the absolute temperature, v is the sliding speed, d is the friction track width, and ΔP is

the change in the partial pressure. This last term could be estimated based on the current change, ΔI , as monitored by the Q-mass based on the relationship

$$\Delta P = C_f \cdot \Delta I \quad (5)$$

where C_f is a calibration coefficient.

Figure 10 plots the hydrogen desorption rate as a function of the sliding distance. The desorption rate increased after a sliding distance of 1.8 km when MAC was used as the lubricant, indicating that this oil required an induction period prior to decomposing on the nascent steel surface. This induction period is defined as the duration from the onset of friction to the start of lubricant decomposition and reflects the relative difficulty in producing a nascent surface [10,15]. That is, the induction period is the duration of the running-in process required to generate a nascent surface. Following this induction period, hydrogen formation would be expected to be stable; however, in fact, it was found to exhibit large fluctuation in these trials. As noted in the discussion of the experimental details, an annealed disk with a hardness of HRC20 and a ball with a hardness of HRC65 were used as the test pieces to accelerate the formation of a nascent surface. In the present work, the resulting severe wear on the disk surface is believed to have led to the unstable hydrogen generation. These results also suggest that MAC would not be a suitable lubricant for severe conditions. The induction period for the ADE was 1.7 km; thus, it was almost the same as that for the MAC. However, the steady state hydrogen desorption rate, especially after a sliding distance of 10 km, was much lower than that for the MAC. Moreover, the relatively minor fluctuations in hydrogen generation confirmed that the ADE was a better lubricant under severe conditions.

Among the PPEs, the 4P2E and R1-4P2E did not exhibit induction periods (Figure 10) and generated hydrogen during the initial friction period. The reasons for these results are presently unclear. The amount of hydrogen produced from the 4P2E was negligible after a sliding distance of 3.5 km, indicating the superior tribochemical stability of this compound. The R1-4P2E showed a similar hydrogen desorption rate to that obtained from the ADE, suggesting that hydrogen was produced largely from the alkyl chains (because the ADE had a $C_{18}H_{37}$ alkyl chain, while the R1-4P2E had a $C_{16}H_{33}$ chain). In contrast, the R2-4P2E exhibited a long induction period of 5.3 km as shown in Figure 10e, meaning that this lubricant would better protect the surface from wear. However, once the surface was worn and the nascent surface was exposed, higher hydrogen generation was observed because of the two $C_{16}H_{33}$ alkyl chains in R2-4P2E.

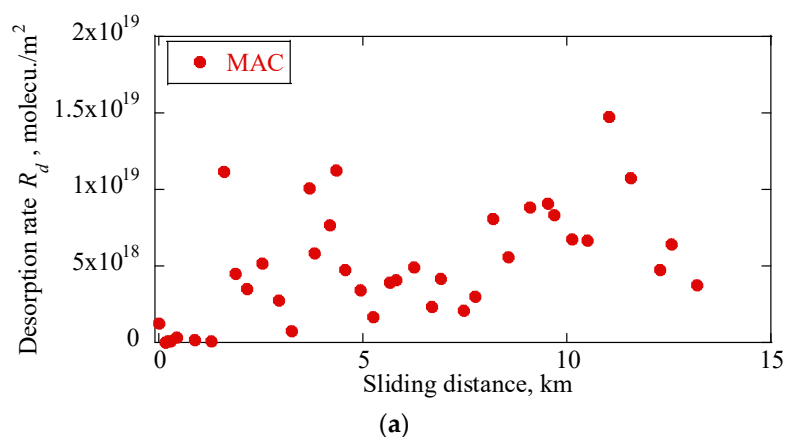
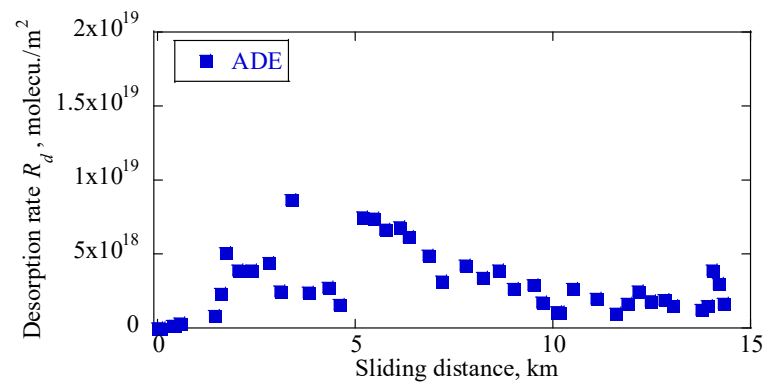
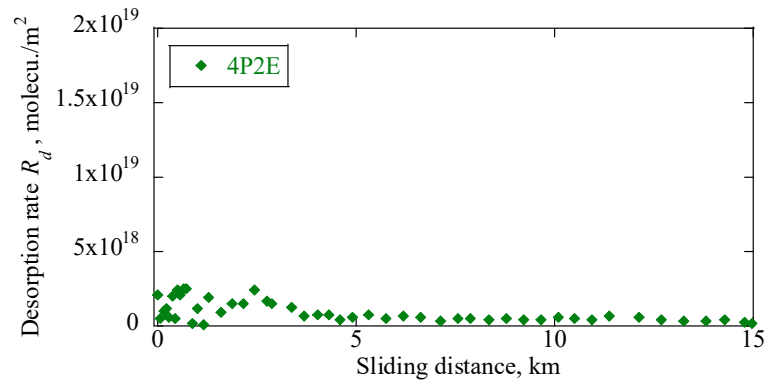


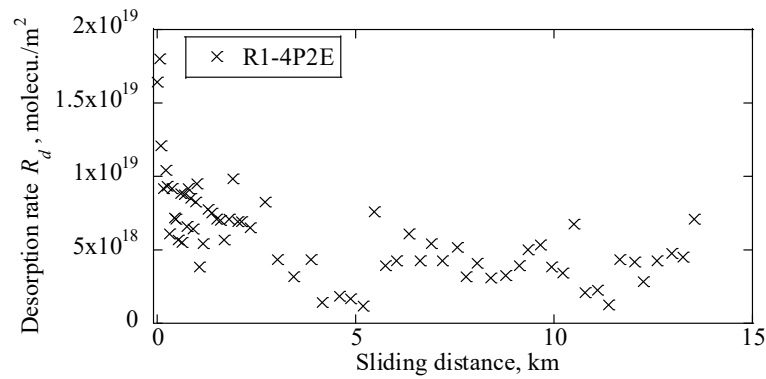
Figure 10. Cont.



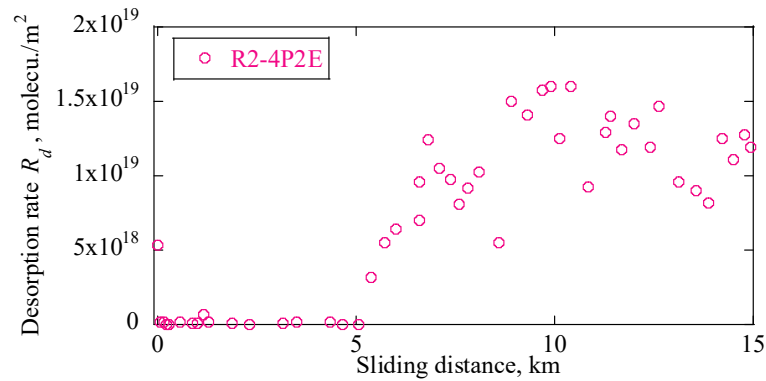
(b)



(c)



(d)



(e)

Figure 10. Desorption of hydrogen during sliding trials with the (a) MAC, (b) ADE, (c) 4P2E, (d) R1-4P2E, and (e) R2-4P2E specimens as functions of the sliding distances.

In addition to hydrogen, methane, ethane, and other low-molecular-weight hydrocarbons were generated during the friction tests, and the associated desorption rates are summarized in Figure 11. The 4P2E, ADE, and R1-4P2E, appearing in the bottom left of this diagram, exhibited high tribochemical stability, while the MAC and R2-4P2E in the top right readily underwent tribochemical decomposition. Alkyl chains therefore appear to have been more easily decomposed on the nascent surface than phenyl ethers. The dissociation energy for C-C bonds in alkyl chains is $347 \text{ kJ}\cdot\text{mol}^{-1}$, while the values for alkyl C-H bonds, C-C bonds in phenyl rings, and $\text{C}_6\text{H}_5\text{-H}$ bonds are 415, 611, and $469 \text{ kJ}\cdot\text{mol}^{-1}$, respectively [35]. Because much less energy is needed to decompose alkyl chains, the MAC and R2-4P2E generated more hydrogen during the friction trials.

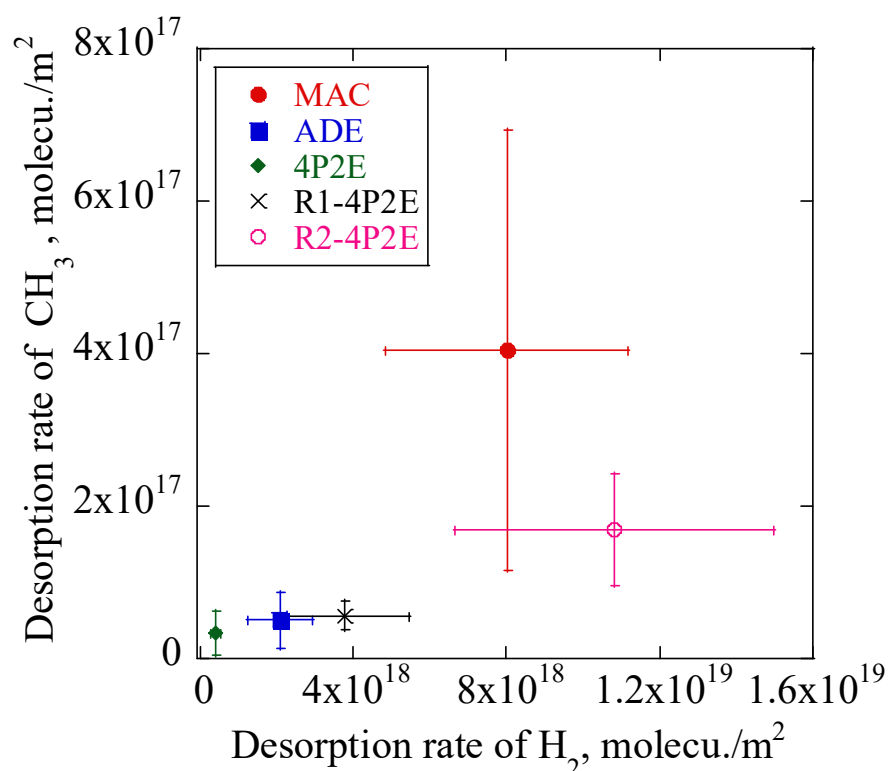


Figure 11. Desorption rates of gaseous product from the various lubricants.

4. Conclusions

Lubricants with thermal and chemical stabilities are needed as an approach to reducing the generation of hydrogen during friction so as to avoid the hydrogen embrittlement of mechanical parts when in motion. In the present work, the friction, wear, and tribochemical stability characteristics of PPEs were evaluated. These materials showed much lower friction coefficients than those for the PAO and ADE samples. The very stable friction coefficients of the PPEs suggest that the running-in process had a minimal effect on friction. The formation of various polymers on the friction track seems to have decreased the friction coefficients. The wear rate was also almost zero for all the PPEs, indicating excellent anti-wear properties. The high viscosity of the PPEs supplied sufficient lubrication between the friction pairs, preventing the surfaces from wearing. The tribochemical stability of the lubricants decreased in the order of $4\text{P2E} > \text{ADE} = \text{R1-4P2E} > \text{R2-4P2E} > \text{MAC}$. The alkyl chains seem to have been more easily decomposed on the nascent surface than the phenyl ethers. In addition, hydrogen generation from the 4P2E was negligible after a sliding distance of 3.5 km. The R1-4P2E specimen exhibited a similar hydrogen desorption rate to that of the ADE because the latter had a $\text{C}_{18}\text{H}_{37}$ alkyl chain, while the former incorporated a $\text{C}_{16}\text{H}_{33}$ chain. Although the R2-4P2E showed a high hydrogen generation rate, its long induction period suggests it could provide suitable wear protection. The incorporation

of alkyl chains increased the likelihood of hydrogen generation; however, the alkylation of these PPEs also increased their mobility while lowering their friction coefficients and producing lower degrees of wear. Thus, this modification could allow such compounds to function as lubricants; considering the widely used lubricant in space systems, MAC, also features multiply-alkyl chains. Multiply alkylation should be important when designing new lubricants.

Author Contributions: Conceptualization, R.L.; methodology, R.L.; experiments, R.L. and M.H.; formal analysis, R.L.; investigation, R.L. and H.T.; visualization, R.L. and H.T.; validation, S.K.; writing—original draft preparation, R.L.; writing—review and editing, R.L., H.T., S.K. and M.H.; supervision, R.L. and H.T. All authors have read and agreed to the published version of the manuscript.

Funding: This research received no external funding.

Institutional Review Board Statement: Not applicable.

Informed Consent Statement: Not applicable.

Data Availability Statement: Not applicable.

Acknowledgments: The authors thank the MORESCO Corporation for supplying the PPEs and ADE.

Conflicts of Interest: The authors declare no conflict of interest.

References

1. Stopher, M.A.; Rivera-Diaz-del-Castillo, P.E.J. Hydrogen embrittlement in bearing steels. *Mater. Sci. Technol.* **2016**, *32*, 1184–1193. [[CrossRef](#)]
2. Lu, R.; Minami, I.; Nanao, H.; Mori, S. Investigation of decomposition of hydrocarbon oil on the nascent surface of steel. *Tribol. Lett.* **2007**, *27*, 25–30. [[CrossRef](#)]
3. Shimotomai, N.; Nanao, H.; Mori, S. Tribochemical reaction of benzene on nascent steel surface and effect of temperature. *Tribol. Online* **2012**, *7*, 54–59. [[CrossRef](#)]
4. Esfahani, E.A.; Soltanahmadi, S.; Morina, A.; Han, B.; Nedelcu, I.; van Eijk, M.C.P.; Neville, A. The multiple roles of a chemical tribofilm in hydrogen uptake from lubricated rubbing contacts. *Tribol. Int.* **2020**, *146*, 106023. [[CrossRef](#)]
5. Kurten, D.; Khader, I.; Kailer, A. Tribochemical degradation of vacuum-stable lubricants: A comparative study between multialkylated cyclopentane and perfluoropolyether in a vacuum ball-on-disc and full-bearing tests. *Lubri. Sci.* **2020**, *32*, 183–191. [[CrossRef](#)]
6. Tanimoto, H.; Tanaka, H.; Sugimura, J. Observation of hydrogen permeation into fresh bearing steel surface by thermal desorption spectroscopy. *Tribol. Online* **2011**, *6*, 291–296. [[CrossRef](#)]
7. Nagumo, M. Hydrogen related failure of steels—A new aspect. *Mater. Sci. Technol.* **2004**, *20*, 940–950. [[CrossRef](#)]
8. Kurten, D.; Khader, I.; Raga, R.; Casajus, P.; Winzer, N.; Kailer, A.; Spallek, R.; Scherge, M. Hydrogen assisted rolling contact fatigue due to lubricant degradation and formation of white etching areas. *Eng. Fail. Anal.* **2019**, *99*, 330–342. [[CrossRef](#)]
9. Tanaka, H.; Ratoi, M.; Sugimura, J. The role of synthetic oils in controlling hydrogen permeation of rolling/sliding contacts. *RSC Adv.* **2021**, *11*, 726–738. [[CrossRef](#)]
10. Lu, R.; Nanao, H.; Kobayashi, K.; Kubo, T.; Mori, S. Effect of lubricant additives on tribochemical decomposition of hydrocarbon oil on nascent steel surfaces. *J. Jpn. Pet. Inst.* **2010**, *53*, 55–60. [[CrossRef](#)]
11. Richardson, A.D.; Evans, M.H.; Wang, L.; Ingram, M.; Rowland, Z.; Llanos, G.; Wood, R.J.K. The effect of over-based calcium sulfonate detergent additives on white etching crack (WEC) formation in rolling contact fatigue tested 100Cr6 steel. *Tribol. Int.* **2019**, *133*, 246–262. [[CrossRef](#)]
12. Lee, F.L.; Harris, J.W. Long-term trends in industrial lubricant additives. In *Lubricant Additives Chemistry and Applications*; Rudnick, L.R., Ed.; CRC Press: Boca Raton, FL, USA, 2009; pp. 615–616.
13. Guarino, F.; Improta, G.; Triassi, M.; Cicatelli, A.; Castiglione, S. Effects of zinc pollution and compost amendment on the root microbiome of a metal tolerant polar clone. *Front. Microbiol.* **2020**, *11*, 1677. [[CrossRef](#)] [[PubMed](#)]
14. Lu, R.; Mori, S.; Kobayashi, K.; Nanao, H. Study of tribochemical decomposition of ionic liquids on a nascent steel surface. *Appl. Surf. Sci.* **2009**, *255*, 8965–8971. [[CrossRef](#)]
15. Lu, R.; Nanao, H.; Takiwatari, K.; Mori, S.; Fukushima, Y.; Murakami, Y.; Ikejima, S.; Konno, T. The Effect of the chemical structures of synthetic hydrocarbon oils on their tribochemical decomposition. *Tribol. Lett.* **2015**, *60*, 27. [[CrossRef](#)]
16. Nozaki, S.; Okasaka, M.; Kubota, Y.; Akabe, S. Trends in automotive instrument and auxiliary bearing technology. *NTN Tech. Rev.* **1996**, *65*, 65–72.
17. Bair, S.; Liu, Y.; Wang, Q.J. The pressure-viscosity of coefficient for Newtonian EHL film thickness with general pezosicous response. *J. Tribol.* **2006**, *128*, 624–631. [[CrossRef](#)]

18. Evans, C.R.; Johnson, K.L. Regimes of traction in elastohydrodynamic lubrication. *Proc. Inst. Mech. Eng. C* **1986**, *200*, 303–312. [[CrossRef](#)]
19. Wolff, R.; Nonaka, T.; Kubo, A.; Matsuo, K. Thermal elastohydrodynamic lubrication of rolling/sliding line contacts. *J. Tribol.* **1992**, *114*, 706–713. [[CrossRef](#)]
20. Ferrari, M.; Zenoni, A.; Lee, Y.; Hayashi, Y. Characterization of a polyphenyl ether oil irradiated at high doses in a TRIGA Mark II nuclear reactor. *Nucl. Instrum. Methods Phys. Res. Sect. B Beam Interact. Mater. At.* **2021**, *497*, 1–9. [[CrossRef](#)]
21. Galmiche, B.; Ponjavic, A.; Wong, J.S.S. Flow measurements of a polyphenyl ether oil in an elastohydrodynamic contact. *J. Phys. Condens. Matter* **2016**, *28*, 134005. [[CrossRef](#)]
22. Herber, J.F.; Joaquim, M.E.; Adams, T. Polyphenyl ethers: Lubrication in extreme environments. *Lubr. Eng.* **2001**, *57*, 9–14.
23. Trivedi, H.K.; Klenke, C.J.; Saba, C.S. Effect of formulation and temperature on boundary lubrication performance of polyphenylethers (5P4E). *Tribol. Lett.* **2004**, *17*, 1–10. [[CrossRef](#)]
24. Otsu, T.; Imado, K. Study on changes in the rheologic properties of EHL film using fluorescence measurements. *Tribol. Lett.* **2018**, *66*, 40. [[CrossRef](#)]
25. Habchi, W.; Vergne, P. A quantitative determination of minimum film thickness in elastohydrodynamic circular contacts. *Tribol. Lett.* **2021**, *69*, 142. [[CrossRef](#)]
26. Itoga, M.; Aoki, S.; Suzuki, A.; Yohsida, Y.; Fujinami, Y.; Masuko, M. Toward resolving anxiety about the accelerated corrosive wear of steel lubricated with the fluorine-containing ionic liquids. *Tribol. Int.* **2016**, *93*, 640–650. [[CrossRef](#)]
27. Hourani, M.J.; Hessell, E.T.; Abramshe, R.A.; Liang, J. Alkylated naphthalenes as high-performance synthetic lubricating fluids. *Tribol. Trans.* **2007**, *50*, 82–87. [[CrossRef](#)]
28. Lu, R.; Morimoto, M.; Tani, H.; Tgawa, N.; Koganezawa, S. Tribological properties of alkyldiphenylethers in boundary lubrication. *Lubricants* **2019**, *7*, 112. [[CrossRef](#)]
29. Ferrari, A.C.; Robertson, J. Raman spectroscopy of amorphous, nanostructured, diamond-like carbon, and nanodiamond. *Philos. Trans. R. Soc. A* **2004**, *362*, 2477–2512. [[CrossRef](#)]
30. Ferrari, A.C.; Robertson, J. Resonant Raman spectroscopy of disordered, amorphous, and diamondlike carbon. *Phys. Rev. B Condens. Matter Mater. Phys.* **2001**, *64*, 075414. [[CrossRef](#)]
31. Chu, P.K.; Li, L. Characterization of amorphous and nanocrystalline carbon films. *Matt. Chem. Phys.* **2006**, *96*, 253–277. [[CrossRef](#)]
32. Sheng, H.; Xiong, W.; Zheng, S.; Chen, C.; He, S.; Cheng, Q. Evaluation of the sp^3/sp^2 ratio of DLC films by RFPECVD and its quantitative relationship with optical band gap. *Carbon Lett.* **2021**, *31*, 929–939. [[CrossRef](#)]
33. Akemann, W.; Otto, A. Vibrational frequencies of C_2H_4 and C_2H_6 adsorbed on potassium, indium, and noble metal films. *Langmuir* **1995**, *11*, 1196–1200. [[CrossRef](#)]
34. Gammage, M.D.; Stauffer, S.; Henkelman, G.; Becker, M.F.; Keto, J.W.; Kovar, D. Ethylene binding to Au/Cu alloy nanoparticles. *Surf. Sci.* **2016**, *653*, 66–70. [[CrossRef](#)]
35. Kameoka, H.; Sonoda, N. *Organic Chemistry*; Kagakudojin: Kyoto, Japan, 1995; pp. 19–21.